Supplementary Information (SI) for ChemComm.
This journal is © The Royal Society of Chemistry 2026

Supporting information

An Endoplasmic Reticulum-Directed ROS Burst Strategy Powered by H_2O_2 Abundance for Chemodynamic/Immuno Tumor Therapy

Ruixiang Liu,† Shurui Weng,† Jiayi Liu, Yaru Cheng, Conghu Liu,* Tailin Xu

College of Chemistry and Environmental Engineering, Institute for Advanced Study, Shenzhen University, Shenzhen, Guangdong 518060, P. R. China

† These authors contributed equally.

*Corresponding author: conghuiliu@szu.edu.cn

1. Experimental Section

1.1 Materials

All of the chemical reagents were used without further purification. Glutathione (GSH) was purchased from Aladdin (Shanghai, China). Silica nanoparticles (20 nm) were procured from Shanghai Yansu Technology Co., Ltd (Shanghai, China). Potassium permanganate ($KMnO_4$), methylene blue (MB), and dichloromethane were purchased from Macklin (Shanghai, China). DSPE-PEG-TSA was purchased from Shanghai Juyijia Biotechnology Co., Ltd.

1.2 Instruments

The TEM images and energy dispersive spectroscopy (EDS) of nanopmaterials were obtained by JEOL JEM-2100 & XMax80 microscope, Japan. The particle size and zeta potential were measured by the Zeta sizer Pro system (Spectris Scientific, Shanghai, China). XRD was measured with a Bruker D8 ADVANCE X. X-ray photoelectron spectroscopy (XPS) spectra were obtained using Thermo Scientific K-AIpha+. The UV-vis absorption spectrum was recorded using a GENESYS 10S spectrophotometer (Thermo Fisher Scientific, USA). •OH was quantified by an ESR spectrometer (EMXplus-6/1, Bruker, Germany). The cytotoxicity measurement was conducted by a microplate reader (Synergy H1, Bioteck). The cell fluorescence imaging experiments were carried out using a confocal laser scanning fluorescence microscope (CLSM, LSM880, CARL ZEISS, Germany). Cell apoptosis and death were analyzed by flow cytometry (NovoCyte, Agilent).

1.3 Synthesis of $MnSiO_3$ NPs

$KMnO_4$ (100 mg) was dissolved in 35 mL of deionized water, and silica nanoparticle templates (5 mL, 18 mg mL^{-1}) with a size of around 20 nm were dispersed in 20 mL of ethanol. Then, the two solutions were mixed and transferred into a Teflon-lined stainless-steel autoclave. After being maintained at 190 °C for 24 h, the resulting solution was naturally cooled to room temperature. The resulting nanoparticles were collected by centrifugation (10 min, 10000 rpm), washed 4-5 times with ethanol and deionized water, and dried to obtain the final $MnSiO_3$ powder.

1.4 Preparation of $MnSiO_3$-T^{ER} NPs

40 mg of $MnSiO_3$ NPs were dispersed in 15 mL of dichloromethane, and 40 mg of DSPE-PEG-TsA

were dispersed in 2 mL of dichloromethane. The two solutions were then mixed and stirred at 600 rpm overnight. The solvent was removed by rotary evaporation to collect the product. The nanoparticles were redissolved in deionized water and purified using Amicon centrifugal ultrafiltration tubes (50 kDa molecular weight) at 13,000 rpm for 2 h to remove free DSPE-PEG-TsA molecules. The resulting product was purified $MnSiO_3$-T^{ER} NPs. For preparing FITC-labeled nanomaterials, the other steps were the same except that the DSPE-PEG-TsA was replaced with DSPE-PEG-FITC-TsA.

1.5 Evaluation of ·OH Generation by MB Degradation

$NaHCO_3$ (200 μL, 25 mM)/5% CO_2 buffer solution, NaCl (200 μL, 50 mM), $MnSiO_3$ NPs (200 μL, 1 mg/mL), and 200 μL of different concentrations of GSH (0, 0.5, 1.0, 5.0, and 10 mM) were mixed and reacted for 1h at 37 °C. The supernatant was collected by centrifugation and then mixed with MB (100 μL, 100 μg/mL) and H_2O_2 (100 μL, 80 mM). After being incubated at 37 °C for 30 min, the mixed solution was measured by a UV-vis spectrophotometer.

1.6 Cell Culture

MCF-7, 4T1, and NHDF cells were incubated in DMEM medium (containing 10% FBS and 1% penicillin-streptomycin, 10,000 U/mL) at 37 °C under 5% CO_2. All of the cell lines used were purchased from BeNa Culture Collection (Henan BeNa Chuanglian Biotechnology Co., Ltd., Henan, China).

1.7 Cellular Uptake Assessment

MCF-7 cells were seeded into plates and incubated overnight. Then, each group was added with FITC-labeled $MnSiO_3$-T^{ER} NPs (50 μg/mL) and incubated for 2 h, 4 h, 6 h, 8 h, 10 h, and 12 h, respectively. After the designated incubation time, the culture medium was removed, and the wells were washed twice with PBS to eliminate non-internalized nanomaterials. The cells were then digested with trypsin and collected by centrifugation. The cells were resuspended in fresh culture medium and passed through a 40 μm cell strainer to prevent cell clumping. The cellular uptake efficiency was evaluated by flow cytometry analysis.

1.8 Cytotoxicity Measurement

MCF-7 and NHDF cells were seeded evenly into 96-well plates at a density of 1×10^4 cells per well,

respectively, and incubated overnight. Then, the culture medium was removed, and $MnSiO_3$ or $MnSiO_3$-T^{ER} solutions at various concentrations (0, 12.5, 25, 50, 100, and 200 μg/mL), prepared in OPTI-MEM medium, were added. Following incubation for 4-6 h, the medium was replaced with fresh DMEM medium. Cells were then cultured for an additional 24 h. Subsequently, 10 μL of CCK-8 solution was added to each well and incubated for 1-4 h. When the OD value of the control group approached 1, absorbance in each well was measured using a microplate reader to assess cell viability under different conditions.

1.9 Intracellular ROS Measurement

Collected cells were seeded onto culture dishes (1×10^5 cells per mL) and incubated overnight. Then the cells were incubated with PBS, $MnSiO_3$, or $MnSiO_3$-T^{ER} NPs (50 μg/mL) prepared in OPTI-MEM medium. Following a 4-hour incubation, the cells were washed three times with PBS. The nuclei were then stained with Hoechst33342 dye (1 mL, 10 μg/mL) by incubating the cells at 37 °C in the dark for 30 min. After removing the staining solution, the cells were washed three times with PBS. Subsequently, DCFH-DA probe (500 μL, 1 mM) was added and incubated in the dark for 30 min. After incubation, the staining solution was removed, and the cells were washed three times with PBS, followed by the addition of 1 mL fresh DMEM medium. Finally, the cells were observed by a confocal laser scanning microscope (CLSM).

1.10 Intracellular ER-Targeting Evaluation

MCF-7 cells were seeded evenly onto dishes at a density of 5×10^4 cells per dish. After cell attachment, 1 mL of FITC-labeled $MnSiO_3$-T^{ER} NPs (50 μg/mL) was added to the dish and incubated for 12 h. Then the cells were washed three times with PBS. Nucleus staining was performed using Hoechst33342 dye (1 mL, 10 μg/mL), followed by incubation at 37 °C in the dark for 30 min. After removing the staining solution, the cells were washed three times with PBS, added with ER-Tracker dye or Lyso-Tracker (1 mL, 1 mM), and incubated in the dark for another 30 min. After being washed 2-3 times with PBS, the cells were observed using a confocal laser scanning microscope.

1.11 Measurement of CHOP Protein Expression in Cells

Cells were seeded into 6-well plates at a density of 2×10^5 cells per well and incubated overnight. After being incubated with 1 mL of $MnSiO_3$ or $MnSiO_3$-T^{ER} NPs (50 μg/mL) prepared in OPTI-MEM

medium for 4 h, the cells were washed 1-2 times with PBS and further incubated for 12 h. Then the cells were lysed using CelLytic M cell lysis buffer. The lysates were centrifuged at 10,000 rpm for 10 min, and the protein concentration in the supernatant was determined using an enhanced BCA protein assay kit. Equal amounts of protein were separated by SDS-PAGE on Bis-Tris gels and transferred onto nitrocellulose membranes. The membranes were then blocked with 5% nonfat milk at room temperature for 2 hours. After blocking, the membranes were incubated overnight at 4 °C with CHOP antibody (1:1000 dilution). Subsequently, membranes were incubated with HRP-conjugated secondary antibodies (1:2000 dilution) for 1 h at room temperature. Protein bands were visualized using an ECL Plus detection kit.

1.12 Tumor Models

All mice used in this study were female Balb/c mice, purchased from the Guangdong Medical Laboratory Animal Center. All animal operations and experiments were conducted in accordance with the Guidelines for the Care and Use of Laboratory Animals in China, and were approved by the Institutional Animal Care and Use Committee of Shenzhen University Medical School. A formal ethical approval certificate for animal experiments was obtained (No. IACUC-202400146). The tumor model was established by subcutaneous injection of murine breast cancer cells (4T1) into the right axillary region of each mouse.

1.13 In vivo Antitumor Effect Evaluation

When the tumor volume reached approximately 50 mm^3 (calculated as $V = 0.5 \times \text{length} \times \text{width}^2$), the mice were randomly divided into three groups for in vivo experiments (5 mice in each group) and intratumorally injected with different formulations every other day for seven doses: (1) PBS (Control); (2) $MnSiO_3$ NPs (20 mg/kg); (3) $MnSiO_3$-T^{ER} NPs (20 mg/kg). The tumor volume and body weight of the mice were recorded every other day to monitor tumor progression under different treatment conditions. On day 14, all mice were sacrificed. Tumors were carefully excised, weighed, photographed, and embedded in paraffin for H&E, TUNEL, and Ki-67 staining. To examine immune responses after treatments, CRT expression, CD86 expression, $CD8^+$ T cell population, and IFN-γ expression in tumor regions were analyzed using immunofluorescence staining. The average fluorescent intensity in sections was measured by ImageJ software.

1.14 Statistical Analysis

Quantitative data are presented as mean ± standard deviation (SD) as indicated in the figure legends. For confocal microscopy image quantification, images were pre-processed in ImageJ software by applying intensity-based thresholding to segment cells. Statistical analyses were performed using OriginPro (learning edition) Software. Comparisons among more than two groups were conducted using one-way analysis of variance (ANOVA), followed by Tukey's post hoc multiple-comparison tests where applicable. A significance level of $\alpha = 0.05$ was used for all analyses. Statistical significance was denoted as ns: not significant, *$p<0.05$, **$p<0.01$, and ***$p<0.001$, as indicated in the figure legends. The sample size (n) for each analysis, representing independent replicates, is reported in the corresponding figure legends, with all experiments performed with $n \geq 3$ unless stated otherwise.

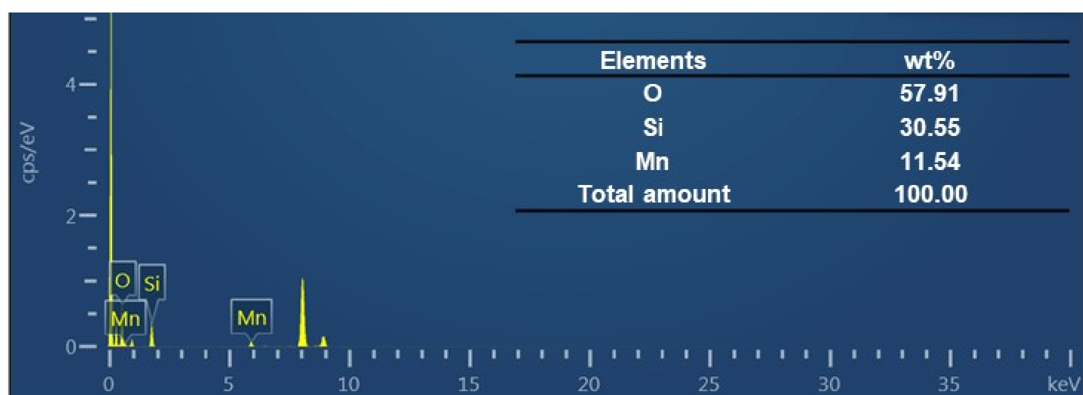

Figure S1. Energy-dispersive spectroscopy (EDS) analysis of $MnSiO_3$ NPs.

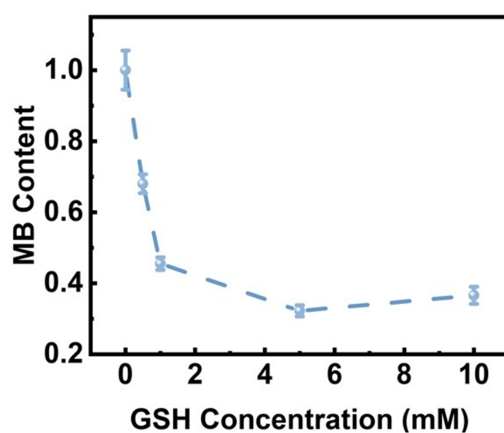

Figure S2. MB degradation rate of $MnSiO_3$ NPs under different GSH concentrations (0-10 mM) in the presence of H_2O_2.

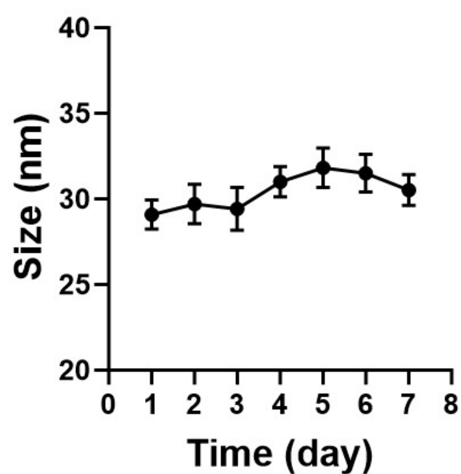

Figure S3. Change in particle size of MnSiO3-TER aqueous suspension stored at 4°C within seven days.

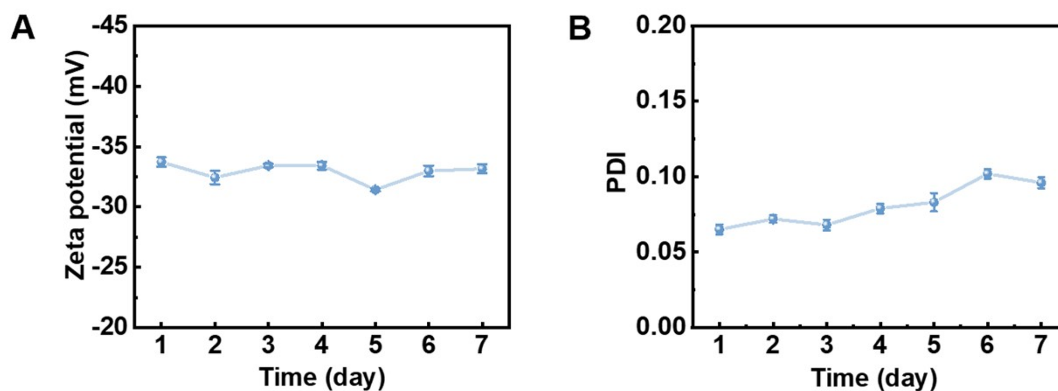

Figure S4. The changes of (A) zeta potential and (B) polydispersity index (PDI) of $MnSiO_3$-T^{ER} aqueous suspensions stored at 4 °C within seven days.

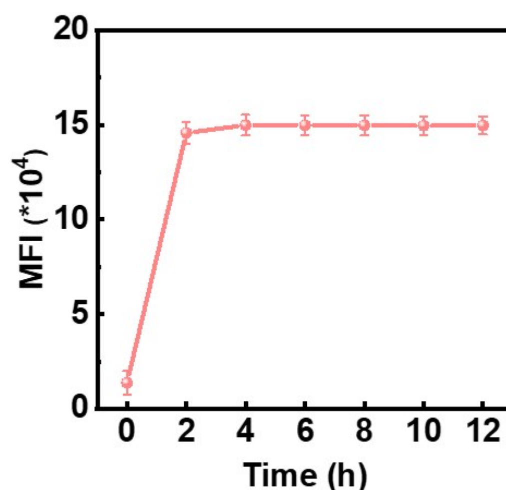

Figure S5. The corresponding mean fluorescence intensity by flow cytometry after different incubation times.

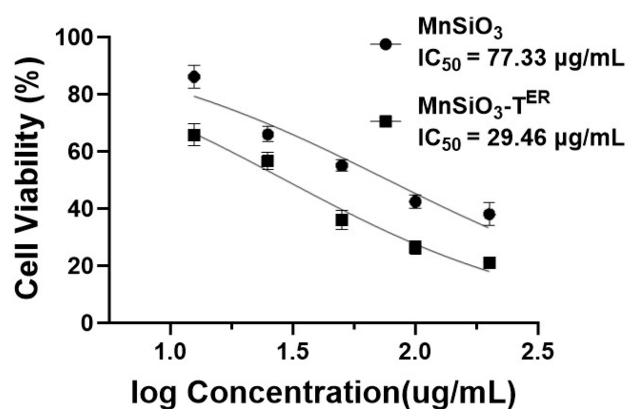

Figure S6. IC_{50} comparison of $MnSiO_3$ and $MnSiO_3$-T^{ER} NPs in MCF-7 cells.

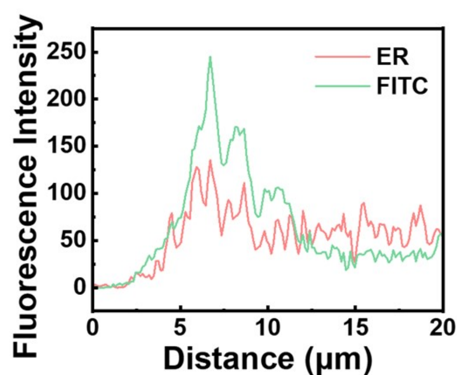

Figure S7. Analysis of fluorescence intensity through co-localization line scanning of ER.

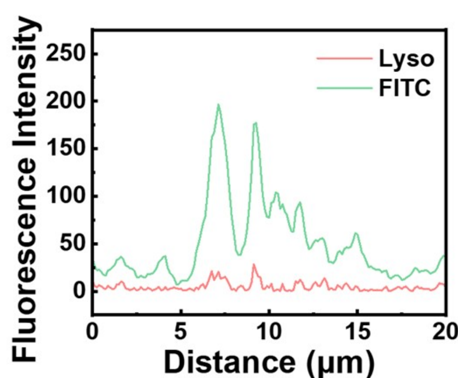

Figure S8. Analysis of fluorescence intensity through co-localization line scanning of lysosomes.

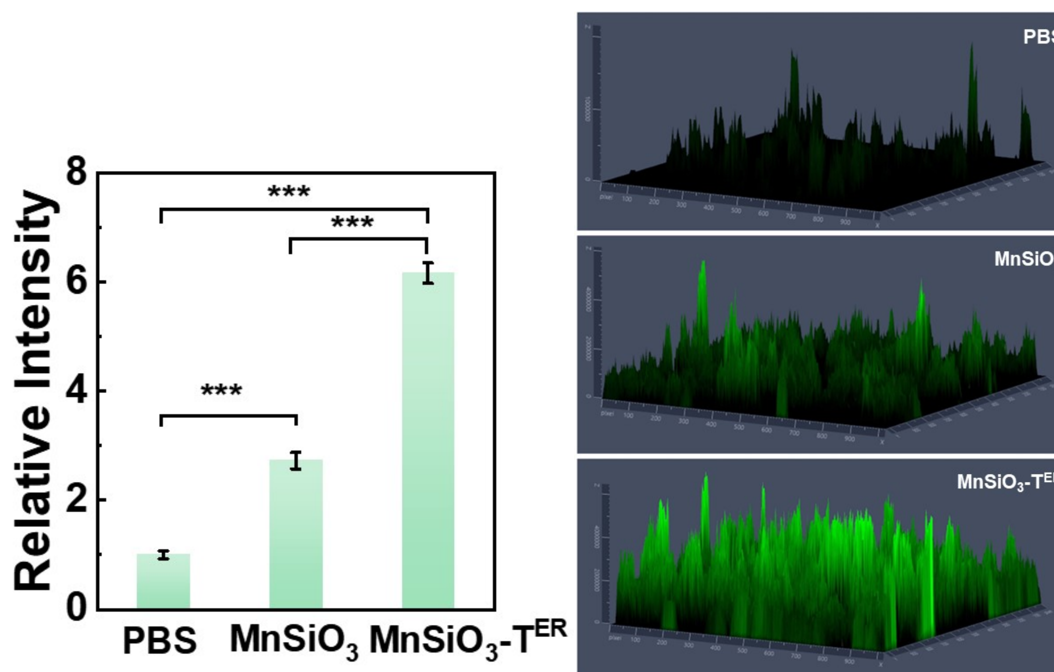

Figure S9. Quantitative analysis (n=3, mean ± SD) and the surface plot images of ROS production in MCF-7 cells. Statistical significance was calculated via one-way analysis of variance test. *$p < 0.05$; **$p < 0.01$; ***$p < 0.001$, ns: not significant.

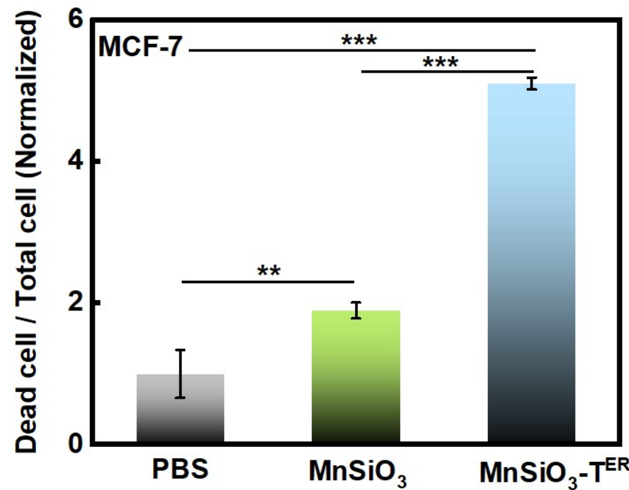

Figure S10. Dead cell/total cell ratio in MCF-7 cells after treatment with PBS, $MnSiO_3$, or $MnSiO_3$-T^{ER}, quantified from Calcein-AM/PI staining. Statistical significance was calculated via one-way analysis of variance test. *p < 0.05; **p < 0.01; ***p < 0.001, ns: not significant.

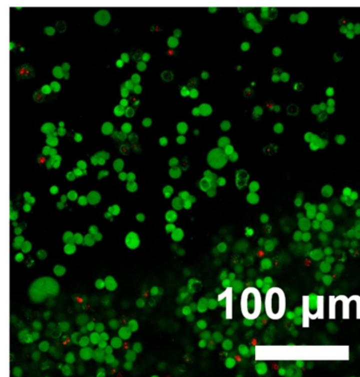

Figure S11. Representative fluorescent imaging of Calcein-AM and propidium iodide (PI) co-stained in NHDF cells with $MnSiO_3$-T^{ER}.

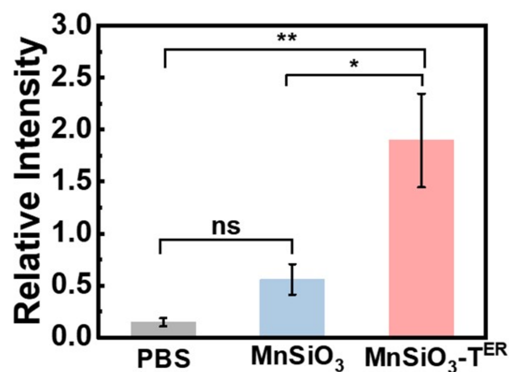

Figure S12. Corresponding quantification analysis after normalization against β-actin (n = 3, mean ± SD). Statistical significance was calculated via one-way analysis of variance test. *p < 0.05; **p < 0.01; ***p < 0.001, ns: not significant.

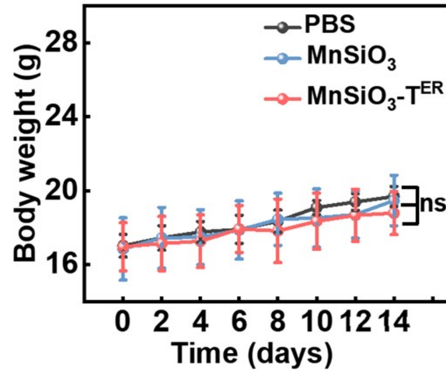

Figure S13. The changes in body weight of tumor-bearing mice after various treatments in 14 days ($n = 5$, mean ± SD). Statistical significance was calculated via one-way analysis of variance test. $^*p < 0.05$; $^{**}p < 0.01$; $^{***}p < 0.001$, ns: not significant.

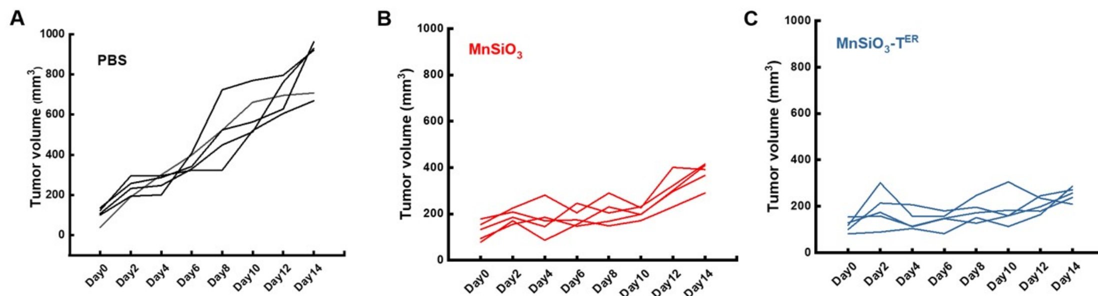

Figure S14. The changes in tumor volume of each mouse in each group during treatment.

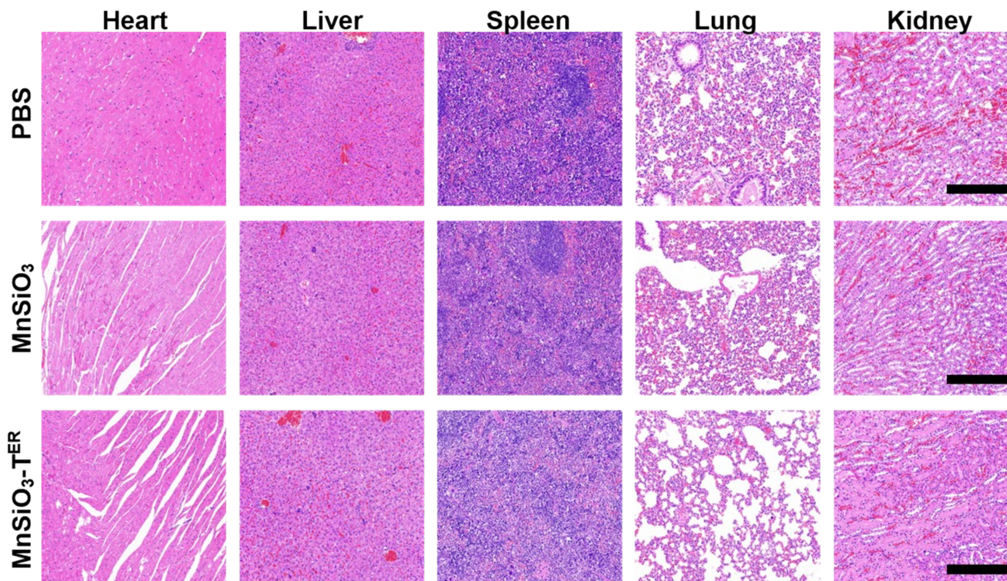

Figure S15. Representative H&E-stained images of organs obtained from mice after 14-day treatment. Scale bar: 100 μm.

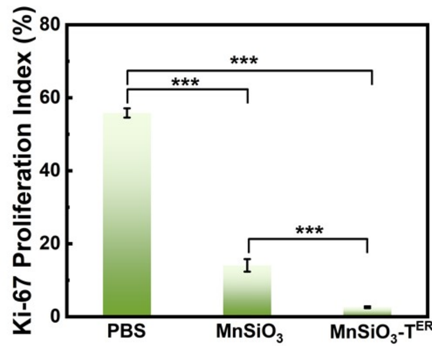

Figure S16. Ki-67 proliferation index among different groups (n = 3, mean ± SD). Statistical significance was calculated via one-way analysis of variance test. *$p < 0.05$; **$p < 0.01$; ***$p < 0.001$, ns: not significant.

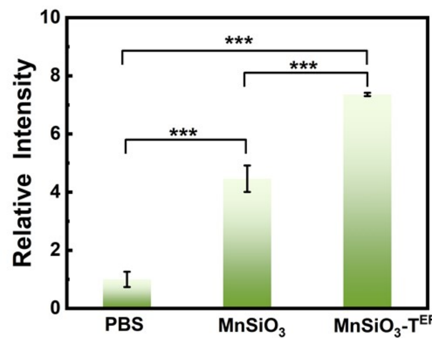

Figure S17. CD86 positive cell rate among different groups(n = 3, mean ± SD). Statistical significance was calculated via one-way analysis of variance test. *$p < 0.05$; **$p < 0.01$; ***$p < 0.001$, ns: not significant.

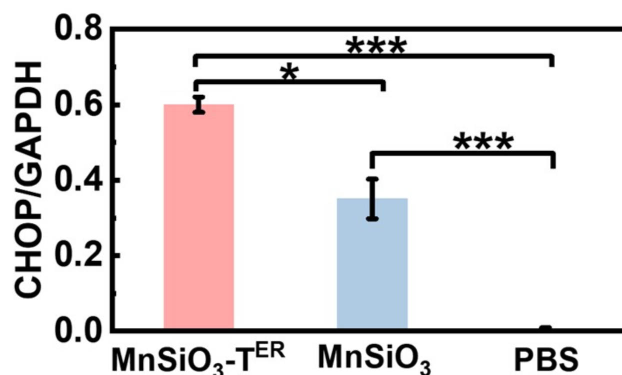

Figure S18. Corresponding quantification normalized by GAPDH (n = 3, mean ± SD). Statistical significance was calculated via one-way analysis of variance test. *$p < 0.05$; **$p < 0.01$; ***$p < 0.001$, ns: not significant.

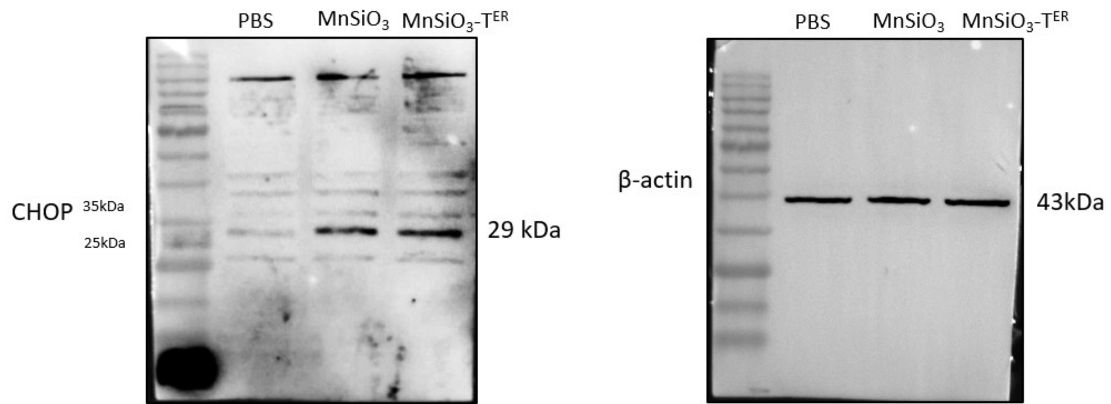

Uncropped gel image for Figure 2f.

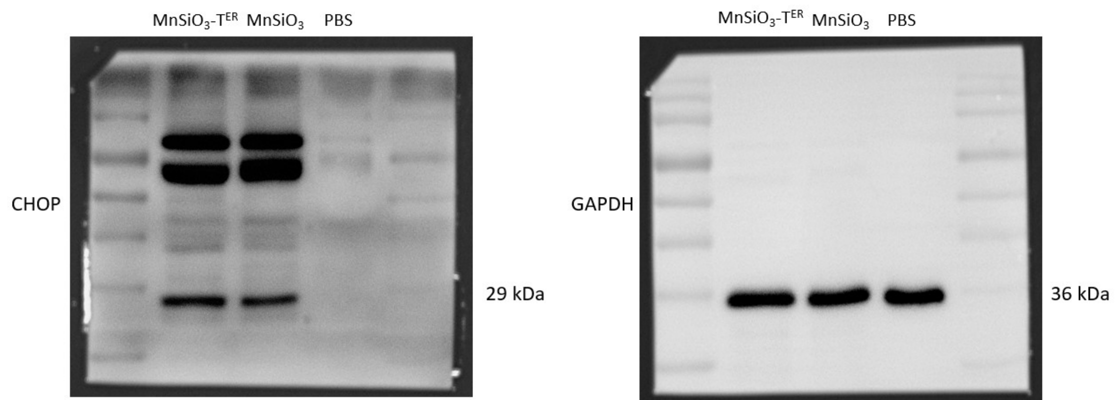

Uncropped gel image for Figure 4c.